Available online at www.sciencedirect.com

SciVerse ScienceDirect

Ceramics International 39 (2013) 4969–4974

CERAMICS
INTERNATIONAL

www.elsevier.com/locate/ceramint

Template-assisted hydrothermal synthesis and photocatalytic activity of novel TiO_2 hollow nanostructures

Guogang Tang[a,b], Shuaishuai Liu[a,b,c], Hua Tang[a,c,*], Du Zhang[a],
Changsheng Li[a], Xiaofei Yang[a,*]

[a] *School of Materials Science and Engineering, Jiangsu University, Zhenjiang, Jiangsu 212013, PR China*
[b] *Department of Chemical Engineering, Zhenjiang College, Zhenjiang, Jiangsu 212003, PR China*
[c] *Key Laboratory of high-end structural materials of Jiangsu Province, Zhenjiang, Jiangsu 212003, PR China*

Received 22 November 2012; received in revised form 26 November 2012; accepted 27 November 2012
Available online 5 December 2012

Abstract

TiO_2 hollow nanostructures were successfully synthesized by a controlled hydrothermal precipitation reaction using Resorcinol–Formaldehyde resin spheres as templates in aqueous solution, and then removal of the RF resins spheres by calcination in air at 450 °C for 4 h. The obtained TiO_2 hollow spheres were characterized by X-ray diffraction, scanning electron microscopy, transmission electron microscopy, N_2 adsorption–desorption analysis, and UV–visible diffuse reflectance spectroscopy. The photocatalytic activity of the as-prepared samples was evaluated by photocatalytic decolorization of rhodamine B aqueous solution at ambient temperature under UV illumination. The results indicated TiO_2 hollow nanostructures exhibit the excellent photocatalytic activity probably due to the unique hollow micro-architectures.

Keywords: TiO_2 hollow nanostructures; Template-assisted hydrothermal; Crystal growth; Photocatalytic activity

1. Introduction

As we well know, TiO_2 is one of the most important n-type wide-band gap semiconductors, which has attracted extensive attention during the past decades for its superior physical and chemical properties [1,2]. Many potential applications such as efficient photocatalysts, photovoltaic cells, photo/electrochromics, photonic crystals, and electrode materials for dye-sensitized solar cells (DSCs) have been extensively investigated [3–7]. These researches indicate TiO_2 exhibit the most suitable for widespread environmental applications compared with other oxide semiconductor photocatalysts because of its biological and chemical inertness, strong oxidizing power, and cost effectiveness. It is well known that photocatalytic activity of TiO_2 materials is concerned with its size, shape and specific surface area. To enhan!ce the properties of TiO_2, various morphologies and structures, including nanotubes, nanorods and porous spheres, of TiO_2 have been synthesized [8–15].

Among these structures, much attention has been paid to the synthesis and study of TiO_2 hollow nanostructures because of their low density, high surface area, good surface permeability as well as large light-harvesting efficiencies. Moreover, it is expected that higher energy conversion efficiency and photocatalytic activity could be achieved using TiO_2 hollow nanostructures as photocatalysts. Currently, the most-applied synthetic strategy for the preparation of hollow structures rely on the use of sacrificial templates, including hard or soft template, and the desired hollow interiors are generated upon the removal of templates by calcination or dissolution [16–19]. Because carbon materials synthesized by hydrothermal carbonization are easy to remove, carbon spheres have been used as sacrificial templates to synthesize hollow

---

*Corresponding authors at: School of Materials Science and Engineering, Jiangsu University, Zhenjiang, Jiangsu 212013, PR China.
Tel./fax: +86 511 8879 0268.
E-mail addresses: hutang79@yahoo.com.cn (H. Tang), xyang@ujs.edu.cn (X. Yang).

0272-8842/$ - see front matter © 2012 Elsevier Ltd and Techna Group S.r.l. All rights reserved.
http://dx.doi.org/10.1016/j.ceramint.2012.11.093

structures. Recently, a general method for the synthesis of metal oxide hollow spheres has been developed using carbon microspheres as templates prepared from saccharide solution. Based on above method, many novel hollow nanostructures composed of materials such as Fe_3O_4, Ni_2O_3, CuO, and ZnS [20,21] have been successfully synthesized.

In this paper, a two-step method for fabricating TiO_2 photocatalyst with hollow nanostructures was developed with using RF resin spheres as templates in aqueous solution. This method is environmentally friendly. The photocatalytic activity of the prepared samples has also been investigated. Moreover, a possible formation mechanism of TiO_2 hollow nanostructures was discussed on the basis of experimental results.

2. Experimental

2.1. Synthesis of resorcinol–formaldehyde resin spheres

Typically, monodisperse RF resins spheres were synthesized by using resorcinol and formaldehyde solution as precursors [22]. In a typical synthesis of the RF resins spheres with 500 nm diameter, ammonia aqueous solution (NH_4OH, 0.1 mL, 25 wt%) was mixed with a solution containing absolute ethanol (EtOH, 8 mL) and deionized water (H_2O, 20 mL), then stirred for more than 1 h. Subsequently, resorcinol (0.2 g) was added and continually stirred for 30 mins. The formaldehyde solution (0.28 mL) then added to the reaction solution and stirred for 24 h at 30 °C, and subsequently heated for 24 h at 100 °C under a static condition in a Teflon-lined autoclave. The solid product was recovered by centrifugation and air-dried at 100 °C for 48 h.

2.2. Synthesis of TiO_2 hollow structures

The TiO_2 hollow structures were prepared as follows: as-prepared RF resins spheres (0.02 g) were suspended in distilled water by continuous stirring. $(NH_4)_2TiF_6$ (1.5 mL, AR grade, SCRC Chemical Co, China) was then added dropwise to the stirred solution for 1 h. The mixture was then transferred into a 100 ml Teflon-lined stainless steel autoclave and sealed, and the autoclave was placed in a pre-heated oven at 60 °C for12 h and naturally cooled down to room temperature. The TiO_2 precursor thus obtained was collected by centrifugation, washed with distilled water and dried under vacuum at 60 °C for 10 h. Finally, the prepared sample was heated in an air atmosphere to a certain temperature (450 °C) and held at this temperature for 4 h to remove the carbon template.

2.3. Characterization

The X-ray diffraction patterns were recorded using a D8 advance (Bruker-AXS) diffractometer with Cu *Ka* radiation ($\lambda = 0.1546$ nm). The morphologies and structures of the samples were characterized by scanning electron microscopy (SEM, JEOL JXA-840A) and transmission electron microscopy (TEM) with a Japan JEM-100CX II transmission electron microscopy. The Brunauer–Emmett–Teller (BET) surface area (S_{BET}) of the powders was analyzed by nitrogen adsorption in an ASAP2020 surface area and porosity analyzer (Micromeritics, USA). All the samples and Degussa P25 were degassed at 180 °C prior to nitrogen adsorption measurements. The BET surface area was determined by a multipoint BET method using the adsorption data in the relative pressure (P/P_0) range of 0.05–0.25. Desorption isotherm was used to determine the pore size distribution via the Barret–Joyner–Halender (BJH) method with cylindrical pore size [23]. The nitrogen adsorption volume at the relative pressure (P/P_0) of 0.994 was used to determine the pore volume and average pore sizes. UV–visible diffused reflectance spectra of the samples were obtained for the dry-pressed disk samples using a UV–visible spectrophotometer (UV2550, Shimadzu, Japan). $BaSO_4$ was used as a reflectance standard in a UV–visible diffuse reflectance experiment. All the measurements were carried out at room temperature.

2.4. Photocatalytic activity test

The evaluation of photocatalytic activity of the prepared samples for the photocatalytic decolorization of RhB aqueous solution was performed at ambient temperature. A 300 W halogen-tungsten through a UV-cutoff filter (> 400 nm), which was positioned 10 cm away from the reactor, was used as a visible light source to trigger the photocatalytic reaction. Experiments were as follows: 0.05 g of the prepared TiO_2 powder was dispersed in a 20 mL of RhB aqueous solution with a concentration of 1×10^{-5} M in a reaction cell. Before illumination, the suspensions were magnetically stirred in the dark for 60 min to ensure the establishment of an adsorption–desorption equilibrium between the photocatalyst powders and RhB. At given time intervals, 3 mL aliquots were sampled and centrifuged to remove photocatalyst powders. The filtrates were analyzed by recording the variations of the absorption-band maximum (553 nm) of RhB in the UV–vis spectrum.

3. Results and discussion

The crystalline phase and size of the TiO_2 hollow nanostructures can be evaluated from X-ray diffraction (XRD) spectra. Fig. 1 shows XRD pattern of the as-prepared sample. It can be seen that all the diffraction peaks match those of anatase TiO_2, which are in good agreement with the values of standard card (JCPDS No. 21-1272). No characteristic peaks of other impurities are detected in the XRD pattern, indicating that TiO_2 hollow nanostructures with high purity and crystalline can be obtained under current synthetic conditions. The

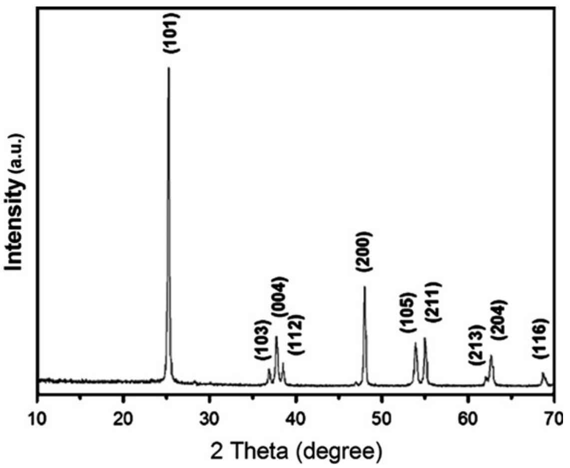

Fig. 1. XRD pattern of the as-prepared TiO_2 hollow nanostructures.

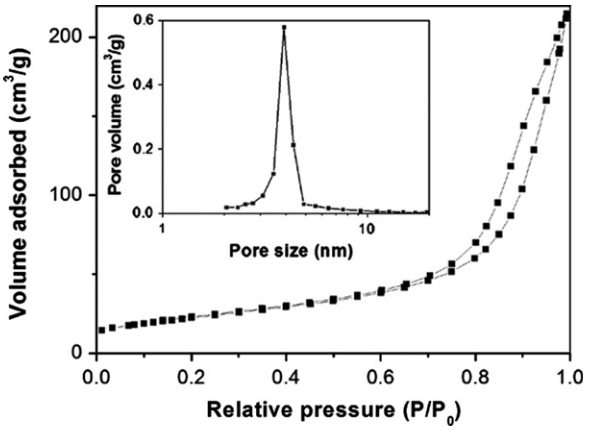

Fig. 2. N_2 adsorption–desorption isotherms and pore size distributions of the as-prepared TiO_2 hollow nanostructures.

broadening of the diffraction peaks can be attributed to the relatively small sizes of the TiO_2 nanocrystals.

Nitrogen adsorption–desorption isotherms were measured to determine the specific surface area and pore volume of the TiO_2 hollow nanostructures. Fig. 2 presents the nitrogen adsorption–desorption isotherm and pore size distribution (inset) of the TiO_2 hollow nanostructures sample. It can be seen that isotherm of the TiO_2 hollow nanostructures sample was of types IV (BDDT classification) [24]. At high relative pressure range from 0.6 to 1.0, the isotherm exhibits a hysteresis loop of type H3 associated with plate-like particles giving rise to narrow slit-shaped pores [24,25], indicating that the powders contain mesopores (2–50 nm) in the TiO_2 hollow nanostructures. The corresponding pore size distribution curve is also shown in Fig. 2 (inset). It can be seen that the hollow TiO_2 nanostructures exhibits a narrow pore size distribution (3–5 nm) with the average pore diameters about 4.2 nm. The S_{BET} and pore volume of as-prepared TiO_2 hollow nanostructures is $80\ \mathrm{m}^2\ \mathrm{g}^{-1}$ and $0.19\ \mathrm{cm}^3/\mathrm{g}$, respectively. According to previous reports [26–29], the mesopores of the TiO_2 hollow nanostructures arise from the interstices among the nanparticles within shells of hollow nanostructures.

The morphology and structure of the samples were further investigated by SEM. Fig. 3(a) show that the RF resins spheres by the Stöber method were approximately spherical with diameters varying between 100 and 200 nm. As shown Fig. 3b, the as-prepared C@TiO_2 core-shell composite nanostructures with diameters ranging from 0.5 μm to 1 μm were synthesized through a hydrothermal process; the size and morphology of the precursor was improved after addition of TiO_2. Fig. 3(c) shows an SEM image of the TiO_2 hollow nanostructures after removal of the RF resins spheres templates by calcination at 450 °C, which reveal that the as-prepared product has a hollow nanostructure with diameters of approximately 0.5 μm–1 μm. The cracked nanostructures with apparent cavities indicate the hollow nature of the products. Fig. 4a is the typical TEM image of the TiO_2 hollow nanostructures which agrees with the results from the above SEM observation. Fig. 4b is a single hollow structure; the thickness of the shell is about 30 nm.

To better understand the underlying the formation mechanism of these TiO_2 hollow nanostructures, the influence of titanium precursor on morphologies of the as-prepared products has been investigated using TBOT as the titanium (Fig. 5). It can be seen that nearly all of TiO_2 particles and carbon spheres are mixed together, and no core-shell structures could be obtained (Fig. 5a). From the magnified SEM images (Fig. 5b), it is clearly found that the sizes of the TiO_2 nanoparticles are about 20–50 nm in diameters. The above results indicate titanium source is believed to the important influent factors for the formation of core-shell composite. Compared with the hydrolysis of TBOT, the hydrolysis of $(NH_4)_2TiF_6$ can easily generate HF in the solution, and these HF are able to erode the surface of carbon spheres template which are favorable for the deposition of TiO_2 nanoparticles on the surface of carbon spheres. Therefore, the hollow nanostructures are readily produced due to the presence of HF in the reaction system.

On the basis of the above experimental results, the template directed deposition of TiO_2 nanoparticles and the template-sacrificial calcination of carbon spheres for the formation process of TiO_2 hollow nanostructures is proposed. The formation process of TiO_2 hollow nanostructures is schematically illustrated in Fig. 6. At the initial stage of reaction, the following reactions take place in the solution:

$$(NH4)_2TiF_6+4H_2O\rightarrow Ti(OH)_4+2NH_4F+4HF \qquad (1)$$

$$Ti(OH)_4\rightarrow TiO_2+2H_2O \qquad (2)$$

In the hydrothermal conditions, $(NH_4)_2TiF_6$ easily decomposed into HF and TiO_2. New-formed HF can erode the surface of RF resin spheres. Subsequently, TiO_2 primary sol particles can deposit preferentially on

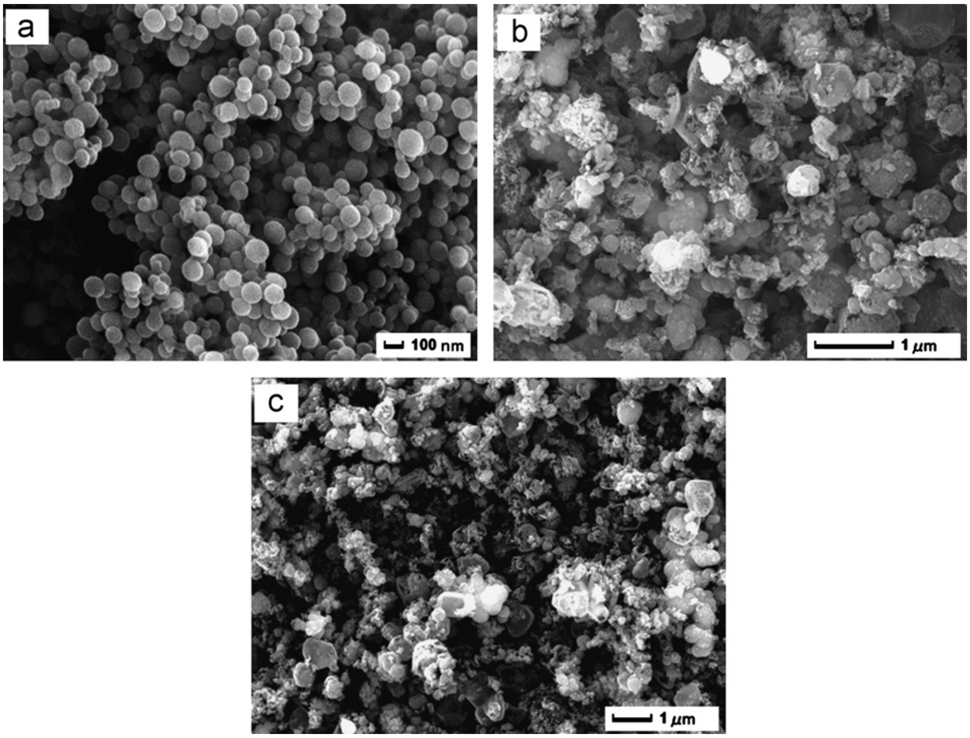

Fig. 3. SEM images of samples obtained after each preparation step (a) RF resins spheres (b) C@TiO_2 precursor (c) TiO_2 hollow nanostructures.

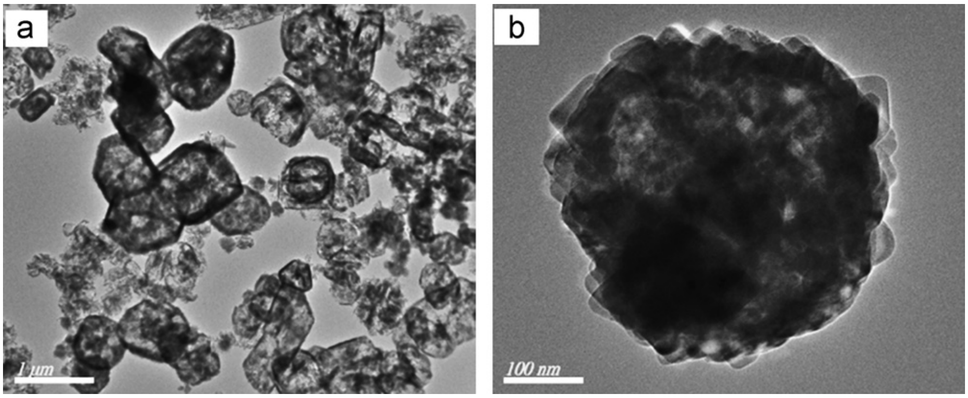

Fig. 4. TEM (a) and HRTEM (b) images of the as-prepared TiO_2 hollow nanostructures.

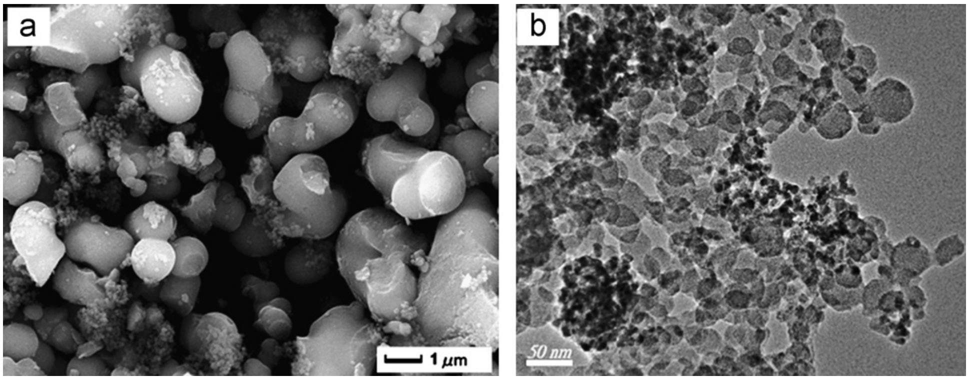

Fig. 5. SEM (a), TEM (b) images of the as-prepared TiO_2 nanoparticles.

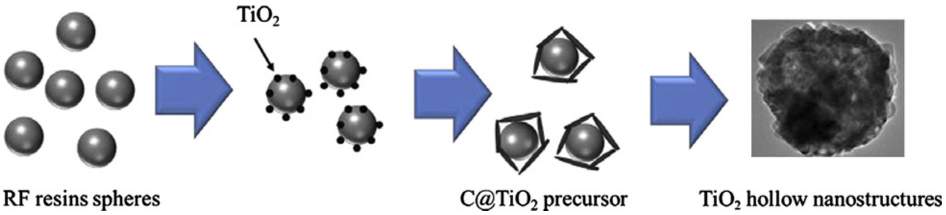

Fig. 6. Schematic illustration of the formation of TiO$_2$ hollow nanostructures.

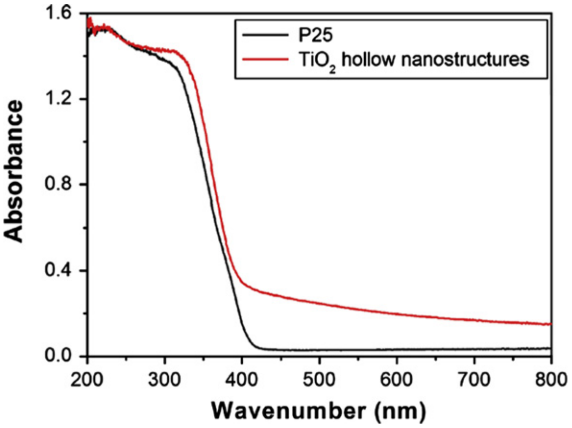

Fig. 7. UV–visible absorption spectra of the TiO$_2$ hollow nanostructures and P25 powders.

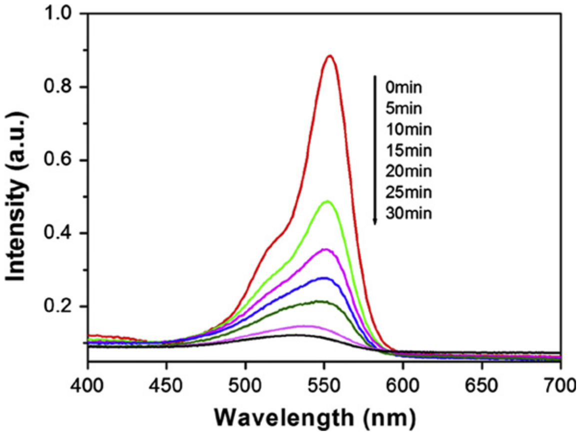

Fig. 8. Absorption changes of RhB aqueous solution at room temperature in the presence of the as-prepared TiO$_2$ under UV irradiation.

the surface of the eroded carbon spheres via adsorption or subsequently hererogeneous nucleation growth, and then assemble together, and spontaneously transform into sheet-like structures around the carbon spheres. With the increase of the reaction time, C@TiO$_2$ core-shell structures are formed from the scabbled TiO$_2$ sheet-like structures through an self-assemble and Ostwald ripening process. Finally, the removal of carbon cores, and densification, cross-link, and phase transformation of TiO$_2$ in the layer via calcinations result in the formation of TiO$_2$ hollow nanostructure.

Fig. 7 shows the UV–visible absorption spectra of the TiO$_2$ hollow nanostructures and Degussa P25 powders. A significant increase in the absorption at wavelengths shorter than 400 nm can be assigned to the intrinsic band gap absorption of TiO$_2$. The absorption spectra of the hollow TiO$_2$ nanostructures show a stronger absorption in the UV–visible light region and a red shift in the band gap transition. The slightly red shift indicated the decrease of band gap energies for the hollow TiO$_2$ samples [23]. The smaller band gap energy means a wider response range of the hollow TiO$_2$ nanostructures sample, and the sample can absorb more photons. This would contribute to an enhanced photocatalytic activity.

The photocatalytic activity of the samples was evaluated by monitoring the degradation of RhB in aqueous solution. Fig. 8 shows the temporal evolution of the absorption spectra of RhB aqueous solution in the presence of TiO$_2$ samples upon exposure to UV illumination light. The absorption peak at 553 nm drops gradually with increasing irradiation time and almost disappears after 30 min, indicating that the TiO$_2$ hollow nanostructures exhibits excellent photocatalytic activity in the degradation of RhB. Fig. 9 shows a comparison of the photocatalytic activities of TiO$_2$ hollow nanostructures and the commercial TiO$_2$ powder (P25). It can be seen from Fig. 9 that the as-prepared products exhibit better photocatalytic activity than that of commercial TiO$_2$. This can be attributed to the increase in specific surface area, the decrease in crystallite size and hollow microarchitecture [29].

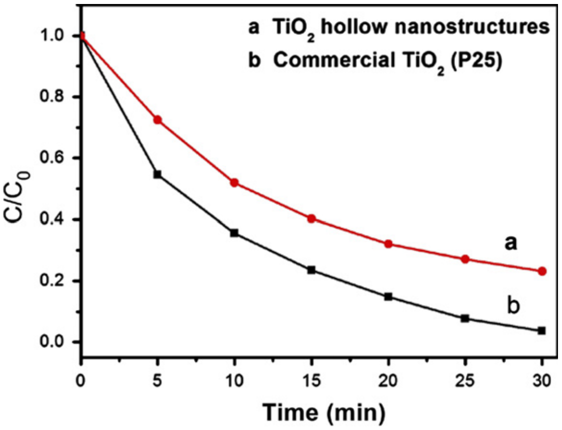

Fig. 9. Comparison of photocatalytic activities of TiO$_2$ hollow nanostructures and commercial TiO$_2$ (P25) for the photocatalytic degradation of RhB aqueous solution at ambient temperature.

4. Conclusions

In summary, TiO_2 hierarchical hollow nanostructures were prepared by a simple one-step low-temperature template method. The hollow structure shows a high photocatalytic activity on the degradation of a methyl RhB solution and can be readily separated from a slurry system after photocatalytic reaction. The approach presented herein can be extended to synthesize fabricate nanoporous metal oxide with controllable structures and compositions, whether we choose suitable nanomaterials as the core or shell components.

Acknowledgments

This work was financially supported by the Open Project of Key Laboratory of Tribology of Jiangsu Province (kjsmcx2011002, kjsmcx1005), the Jiangsu National Nature Science Foundation (BK2011534), and the Senior Intellectuals Fund of Jiangsu University (09JDG009).

References

[1] C.Y. Song, W.J. Yu, B. Zhao, et al., Efficient fabrication and photocatalytic properties of TiO_2 hollow spheres, Catalysis Communications 10 (2009) 650–654.

[2] E. Sahinkaya, N. Uzal, U. Yetis, et al., Biological treatment and nanofiltration of denim textile wastewater for reuse, Journal of Hazardous Materials 153 (3) (2008) 1142–1148.

[3] H.L. Zhou, Z. Zou, S. Wu, et al., Rapid synthesis of TiO_2 hollow nanostructures with crystallized walls by using CuO as template and microwave heating, Materials Letters 65 (2011) 1034–1036.

[4] A.R. Tao, S. Habas, P.D. Yang, Shape control of colloidal metal nanocrystals, Small 4 (3) (2008) 310–325.

[5] P.D. Yang, D.Y. Zhao, D.I. Margolese, et al., Block copolymer templating syntheses of mesoporous metal oxides with large ordering lengths and semicrystalline framework, Chemistry of Materials 11 (10) (1999) 2813–2826.

[6] X. Wang, B. Huang, Z. Wang, X. Qin, et al., Synthesis of anatase TiO_2 tubular structures microcrystallites with a high percentage of {001} Facets by a simple one-step hydrothermal template process, Chemistry-A European Journal 1 (24) (2010) 7106–7109.

[7] X. Lu, F. Huang, J. Wu, et al., Intelligent hydrated-sulfate template assisted preparation of nanoporous TiO_2 spheres and their visible-light application, ACS Applied Materials and Interfaces 3 (2) (2011) 566–572.

[8] S. Zhang, C.Y. Liu, Y. Liu, et al., Fabrication of micrometer-scale anatase-phase TiO_2 congeries assembled with hollow spheres, Journal of the American Ceramic Society 91 (6) (2008) 2067–2070.

[9] W.H. Shen, Y.F. Zhu, X.P. Dong, et al., A new strategy to synthesize TiO_2-hollow spheres using carbon spheres as template, Chemistry Letters 34 (6) (2005) 840–841.

[10] J.G. Yu, X.J. Zhao, Q.N. Zhao, Preparation and characterization of TiO_2 nanometerthin films by sol–gel process, Acta Physico-Chimica Sinica 16 (9) (2000) 792–797.

[11] J.G. Yu, H.G. Yu, Hydrothermal synthesis and photocatalytic activity of mesoporous titania hollow microspheres, Journal of Physics and Chemistry of Solids 69 (5–6) (2008) 1147–1151.

[12] J.S. Chen, Y.L. Tan, C.M. Li, et al., Constructing hierarchical spheres from large ultrathin anatase TiO_2 nanosheets with nearly 100% exposed (001) facets for fast reversible lithium storage, Journal of the American Chemical Society 132 (17) (2010) 6124–6130.

[13] H. Lin, L. Li, M. Zhao, et al., Synthesis of high-quality brookite TiO_2 single-crystalline nanosheets with specific facets exposed: tuning catalysts from inert to highly reactive, Journal of the American Chemical Society 134 (20) (2012) 8328–8331.

[14] B. Liu, E.S. Aydil, Growth of oriented single-crystalline rutile TiO_2 nanorods on transparent conducting substrates for dye-sensitized solar cells, Journal of the American Chemical Society 131 (11) (2009) 3985–3990.

[15] Y. Dai, C.M. Cobley, J. Zeng, et al., Synthesis of anatase TiO_2 nanocrystals with exposed {001} facets, Nano Letters 9 (6) (2009) 2455–2459.

[16] Iijima, Helical microtubules of graphitic carbon, Nature 354 (1991) 56–58.

[17] Q. Wang, H. Li, L.Q. Chen, et al., Monodispersed hard carbon spherules with uniform nanopores, Carbon 39 (14) (2001) 2211–2214.

[18] X. Zhang, Y. Sun, X. Cui, et al., Carbon-incorporated TiO_2 microspheres: facile flame assisted hydrolysis of tetrabutyl orthotitanate and photocatalytic hydrogen production, International Journal of Hydrogen Energy 37 (2) (2012) 1356–1365.

[19] Q. Zhang, W. Li, S.X. Liu, Controlled fabrication of nanosized TiO_2 hollow sphere particles via acid catalytic hydrolysis/hydrothermal treatment, Powder Technology 212 (2011) 145–150.

[20] B. Hu, K. Wang, L.H. Wu, et al., Engineering carbon materials from the hydrothermal carbonization process of biomass, Advanced Materials 22 (7) (2010) 813–828.

[21] S.X. Liu, J. Sun, Z.H. Huang, Carbon spheres/activated carbon composite materials with high Cr (VI) adsorption capacity prepared by a hydrothermal method, Journal of Hazardous Materials 173 (2010) 377–383.

[22] J. Liu, S.Z. Qiao, H. Liu, et al., Extension of the stöber method to the preparation of monodisperse resorcinol–formaldehyde resin polymer and carbon spheres, Angewandte Chemie-International Edition 50 (2011) 5947–5951.

[23] J.G. Yu, J.C. Yu, M.P. Leung, et al., Effects of acidic and basic hydrolysis catalysts on the photocataytic activity and microstructures of bimodal mesoporous titania, Journal of Catalysis 217 (2003) 69–78.

[24] J.G. Yu, S.W. Liu, H.G. Yu, Microstructures and photoactivity of mesoporous anatase hollow microspheres fabricated by fluoride-mediated self-transformation, Journal of Catalysis 249 (2007) 59–66.

[25] J.G. Yu, Y. Su, B. Cheng, Template-free fabrication and enhanced photocatalytic activity of hierarchical macro-/mesoporous titania, Advanced Functional Materials 17 (2007) 1984–1990.

[26] J.G. Yu, X.X. Yu, B. Huang, et al., Hydrothermal synthesis and visible-light photocatalytic activity of novel cage-like ferric oxide hollow spheres, Crystal Growth and Design 9 (2009) 1474–1480.

[27] J. Yu, J. Zhang, A simple template-free approach to TiO_2 hollow spheres with enhanced photocatalytic activity, Dalton Transactions 39 (2010) 5860–5867.

[28] J.G. Yu, X.X. Yu, Hydrothermal synthesis and photocatalytic activity of zinc oxide hollow spheres, Environmental Science and Technology 42 (2008) 4902–4907.

[29] J. Yu, W. Liu, H. Yu, A. One-Pot, Approach to hierarchically nanoporous titania hollowmicrospheres with high photocatalytic activity, Crystal Growth and Design 8 (3) (2008) 930–934.